Senior Thesis

Ground Penetrating Radar in Tree Root Detection

by
Teresa Van Vleck
1999

Submitted as partial fulfillment of
the requirements for the degree of
Bachelor of Science in Geological
Sciences at The Ohio State University,
Spring Quarter, 1999

Approved by:

Dr. Jeffrey Daniels

Table of Contents

List of Figures

Abstract

A ground penetrating radar (GPR) survey was conducted adjacent to a tree at the Brookhaven National Laboratory in Long Island, New York. This data was used to test the effectiveness of GPR to detect tree roots in the subsurface. Using the Radacal and Brick-of -Bytes (BOB) programs 2-D and 3-D images were produced. The objective of this case study is to test the ability of Ground Penetrating Radar to image tree roots in the shallow subsurface, and to compare and contrast the effect of dipole antenna system position to direction of traverse.

Introduction

The use of GPR for tree root detection has applications in botany, horticulture, forestry and engineering. Botanists and horticulturists create models of root geometry based on the size of the plant above ground. This can provide inaccurate data because root morphology can stray from the statistical model due to environmental factors (Wu, 1988). Foresters and engineers are primarily interested in the affect of roots on slope stability (Wu, 1988). Theory and research shows that plant roots aid in slope stability by strengthening the soil (Geotechnical Engineering). Engineers use stability analysis to evaluate soil strength and determine if safety conditions have been met (Geotechnical Engineering). Estimation of the strength of a soil reinforced by roots calls for a knowledge of the number, diameter, orientation and strength of roots (Wu, 1988). With the use of GPR and 3-D imaging a more comprehensive picture of root morphology can be determined with out relying on statistical models or excavation.

Ground Penetrating Radar

GPR is an electromagnetic technique used to detect physical changes in the subsurface. It has a wide range of applications from environmental and engineering to forensics. Field operation of a GPR system is not complicated and concentrated data can be acquired quickly. Basic radar equipment includes a signal generator, transmitting and receiving antenna, and a receiver. Data collection entails towing the equipment along evenly spaced profile lines while recording continuously or at discrete intervals. A person or all-terrain vehicle typically pulls the equipment and measurements are made at equal intervals along the traverse line.

While dragging the equipment along the ground a signal generator applies a time-domain pulse to the transmitting antenna. The transmitter, pointing into the ground, then emits an electromagnetic wave with wavelength from approximately 25 MHz to 1 GHz (Daniels, 1996). The wave propagates through the subsurface until encountering an object or interface with contrasting electrical properties. Polarization and reflection of the wave occurs if the material is primarily a dielectric with low loss (Roberts and Daniels, 1996). The receiver scans at a fixed rate, each scan lasting as long as the desired two way travel time, which can be set from a few tens to several thousand Ns (Reynolds, 1997).

The antenna system can be either monostatic or bistatic. Monostatic mode occurs when a single antenna is used as both a transmitter and receiver. Bistatic mode uses two antennas, one working as a transmitter and the other as a receiver. In bistatic mode the transmit and receive antennas can be oriented parallel to one another (a co-pole configuration) or the transmit and receive antennas can be oriented orthogonal to one another (a cross-pole configuration). Signals acquired are displayed as traces with the vertical axis measuring the two-way travel time and the horizontal axis measuring surface position. By combining the traces from one profile line a shallow, high-resolution cross section of the subsurface can be drawn. The depth of an object or interface can then be resolved if the velocity of the material (Vm) through which the wave is propagating is known

$$D = t * (Vm) / 2,$$

where D is the depth and t is the two-way travel time (Daniels, 1996).

To find the velocity of the material the permittivity of the rock or soil in the subsurface must be known. The relative permittivity of the material is the ratio of the permittivity of the material divided by the permittivity of air

$$\in r = \in m / \in o,$$

where $\in r$ is the relative permittivity, $\in m$ is the permittivity of the rock or soil, and $\in o$ is the permittivity of free space (Daniels, 1996).

The velocity of the material can then be determined from the equation

$$Vm = Vo / \sqrt{\in r},$$

where Vo is the velocity of a radar wave in air (Daniels, 1996). With this information the depth can be determined.

Methods

The data in this study was acquired from the Brookhaven National Laboratory in Long Island, New York by Professor Jeffrey Daniels and Dr. Lucian Wielopolsk: of the Brookhaven National Laboratory. The data was taken over sandy soil adjacent to a tree. An 85 cm x 150 cm area was surveyed. Each profile line is 85 cm long and spaced 2 cm apart resulting in 75 lines. All lines were run in the same direction using a 1.5 GHz bistatic co-pole antenna system. Two data sets were obtained. The first set had the transmitter and receiver oriented perpendicular to the direction of traverse. The second set of data had the dipoles oriented parallel to traverse direction. (Figure 1). The data will compare these two orientations.

Data Processing

2-D data processing was performed using the Radacal program. For the field data to be used on the Silicon Graphics, Inc. (SGI) workstation, a process of byte swapping was first applied. The second step in processing was line length standardization. Line

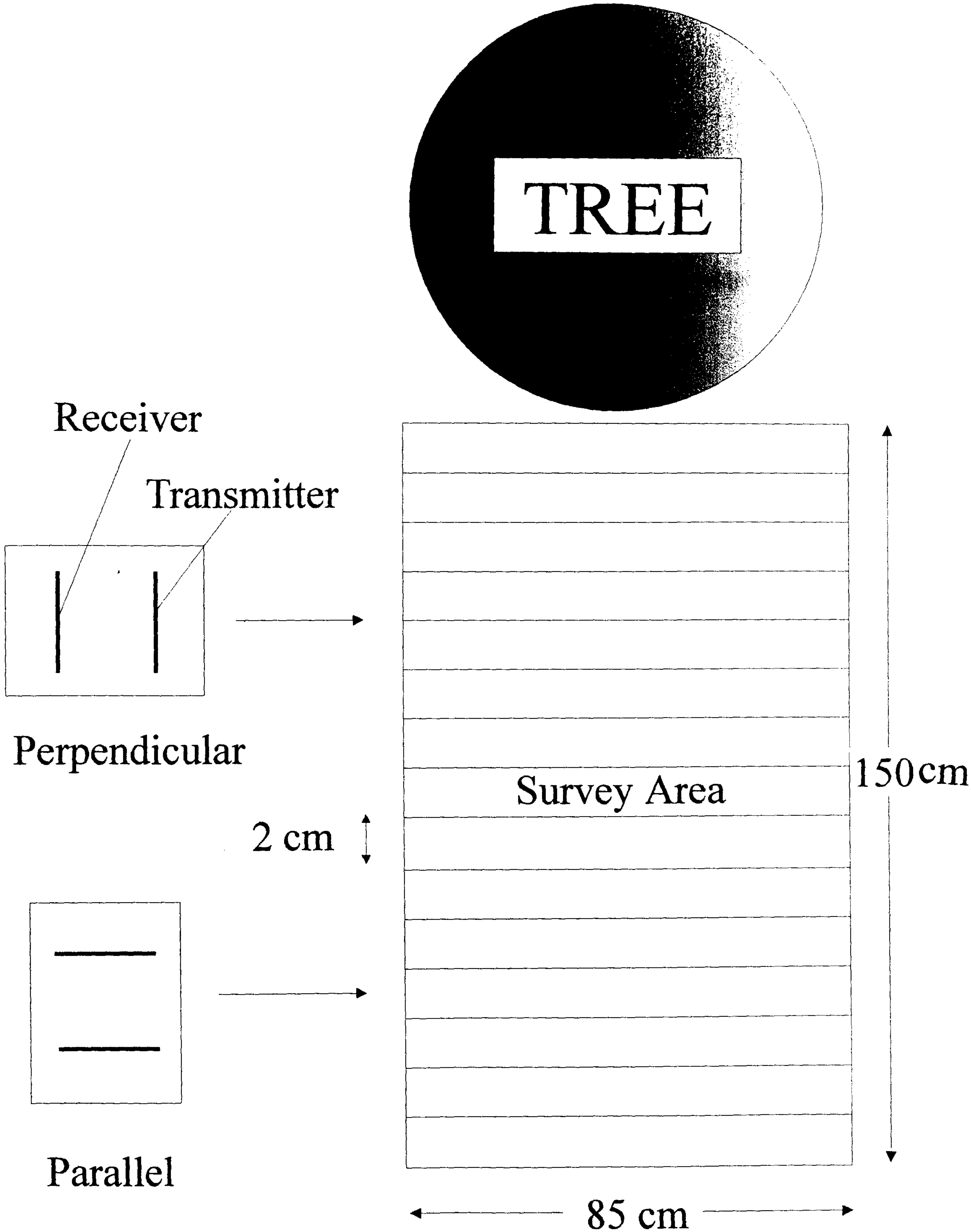

Figure 1. General view of survey area and antenna orientation

length standardization is necessary because the number of traces actually recorded in the field does not always agree with the number of traces assumed recorded per unit distance. In this case 4.54 traces/cm was desired for both data sets. Next, gain processing was performed. Gain processing can increase or decrease the amplitude of the GPR signal according to a selected function of time. With this data, increasing amplitude with time enhanced only background noise so no gain was used. At this point 2-D profiles of lines 10,30, 50, 70, 90, 110, 130, and 150 were created for both data sets (Figures 2-9). To prepare the data for 3-D volume display byte-scaling was applied with user-defined amplitude cutoff values. For the co-pole perpendicular data an amplitude cutoff range between –8000 and 8000 relative amplitude units was used. For the co-pole parallel data an amplitude cutoff range of between -7500 and 7500 relative amplitude units was used. The resulting output was then imaged as a 3-D volume pixel based display using the BOB display program program.

Results

Dipole antennas emit electromagnetic waves with the electric field oriented parallel to the long axis of the antenna (Roberts and Daniels, 1996). This orientation is called linear polarization (Kraus, 1984). The polarization direction of the transmitted signal impacts how waves are scattered from objects or interfaces in the subsurface. The electrical properties, size, shape, orientation and depth of the scatterer relative to the incident polarized field determines the orientation of the reflected polarized field. A dipole receiver will detect the reflected field when it is oriented parallel to the transmitted polarized field (Roberts and Daniels, 1996). A bistatic co-pole antenna system oriented perpendicular to traverse direction is the most sensitive to cylinders aligned parallel to the long axes of the antenna (Roberts and Daniels, 1996). If the reflected polarized field is not parallel to the transmitted polarized field it is referred to as depolarized and the scattered field generally will not be detected by the co-pole antenna system. The tree root targets are assumed to be primarily oriented orthogonal to the traverse direction of the antenna system and one would expect the antenna system operating perpendicular to traverse direction to produce a superior image.

2-D Results

Figures 2-9 show the profile lines located at 10 cm, 30 cm, 50 cm, 70 cm, 90 cm, 110 cm, 130 cm, and 150 cm along the grid of lines shown in figure 1. The co-pole perpendicular image is at the top of the page and the co-pole parallel image is at the bottom of the page. Overall, the co-pole perpendicular images have stronger and better-defined hyperbolas than the co-pole parallel images. This indicates that the co-pole perpendicular system is receiving a stronger reflected polarized field than the co-pole parallel.

In Figure 2, profile line at 10 cm, both images show an anomaly between 10 cm and 30cm and at approximately 4 ns. The co-pole perpendicular image also has a hyperbola at 50 cm and approximately 15 ns, which is absent in the co-pole parallel image. In figure 3, profile line at 30 cm, there is an anomaly in both images at 20 cm and approximately 2.5 ns. The anomaly in the co-pole perpendicular image is better defined than the co-pole parallel. In figure 4, profile line 50 cm, there are corresponding anomalies in the co-pole perpendicular and co-pole parallel images between 60 cm and

80 cm and at approximately 5 ns. Once again the hyperbola in the co-pole perpendicular image is better defined. In figure 5, profile line at 70 cm, the co-pole perpendicular image has a very strong hyperbola between 20 cm and 40 cm and at 5 ns. In the co-pole parallel data the hyperbola is not seen. This would indicate a root oriented orthogonal to traverse direction. In figure 6 and figure 7, profile lines at 90 cm and 110 cm respectively, strong hyperbolas occur in the co-pole perpendicular images between 20 cm and 40 cm and at approximately 5 ns. In figure 6 no corresponding hyperbola is seen in the co-pole parallel image. However in figure 7 a faint corresponding hyperbola is seen. This indicates that the tree roots' orientation has changed, and is no longer orthogonal.

As stated above the co-pole antenna system generally does not detect depolarized or scattered fields. This can prevent target identification from 2-D profile line data. If the co-pole data is acquired as a 2-D grid, then the orientation of the target may be seen in 3-D visual displays that show the spatial variation in the scattered field produced by the target (Roberts and Daniels, 1996).

3-D Results

Figures 12 and 13 show 3-D displays of the co-pole perpendicular and co-pole parallel data sets respectively. In each display a selective time/depth slice has been taken from the 3-D voxel (volume-pixel) display of the survey area and enlarged. In the co-pole perpendicular time slice "crossing" tree roots aligned primarily orthogonal to the transmitter and receiver can be seen. In the co-pole parallel display the roots are not visible. In figures 10 and 11 three time slices have been taken from the 3-D display of the survey area. In Figure 10 the crossing, elongated roots on the left side of the display are clearly visible and in figure 11 possible non-orthogonal roots on the left side of the display may be seen. Figures 10 and 11 also show the decrease of anomalies with depth as would be expected with a tree root system. Figure 14 shows the co-pole perpendicular display divided into four distance slices. With this display the anomalies appear deeper the further the distance from the tree. This too would be expected from a typical tree root system.

Interpretation of GPR data requires an experienced practitioner who can discriminate between target reflections and undesirable scatterers (Roberts and Daniels, 1996). In this case the data could have been interpreted and processed in a different and possibly more effective way.

Conclusion

From GPR tree root data collected at the Brookhaven National Lab both 2-D and 3-D images of roots in the subsurface were produced. Comparison of these images shows that the orientation of dipole position to direction of traverse affects the ability to interpret targets in the subsurface. Linear polarization of the incident electromagnetic field and the orientation of the target with respect to the field determine the ability of the co-pole antenna system to receive reflected energy. In this case the dipoles oriented perpendicular to traverse direction were able to produce a superior image of the roots. The dipoles oriented parallel to traverse direction produced virtually no strong hyperbolas in the 2-D data but possibly produced root images that were non-orthogonal in the 3-D displays. As with any interpretation the results are only as good as the experience and knowledge of the practitioner.

References

Daniels, D.J. Surface-Penetrating Radar. United Kingdom: Institution of Electrical Engineers, 1996.

Daniels, Jeffrey J., and Grumman, David L. Development of a Three Dimensional Subsurface Imaging Computer Display System for Using Ground Penetrating Radar to Locate Buried Substances. Chicago: U.S. Environmental Agency, 1996.

Halliday, David., Resnick, Robert., and Walker, Jearl. Fundamentals of Physics Extended. 5th ed. New York: Wiley, 1997.

Kraus, J.B. Electromagnetics. New York: McGraw-Hill, 1984.

Peters, Leon Jr., Daniels, Jeffrey J., and Young, Jonathon D. Ground Penetrating Radar as a Subsurface Environmental Sensing Tool. Proceedings of the IEEE 82, (1994): 1802-1822.

Reynolds, John M. An Introduction to Applied and Environmental Geophysics. England: Wiley, 1997.

Roberts, Roger L., Daniels, Jeffrey J. Analysis of GPR Polarization Phenomena. Journal of Environmental and Engineering Geophysics 1 (1996): 139-157.

Wu, Tien H. A Statistical Model of Root Geometry. Forest Science 34 (1988): 980-997.

Wu, Tien H. Slope Stabilization Using Vegetation. Geotechnical Engineering.

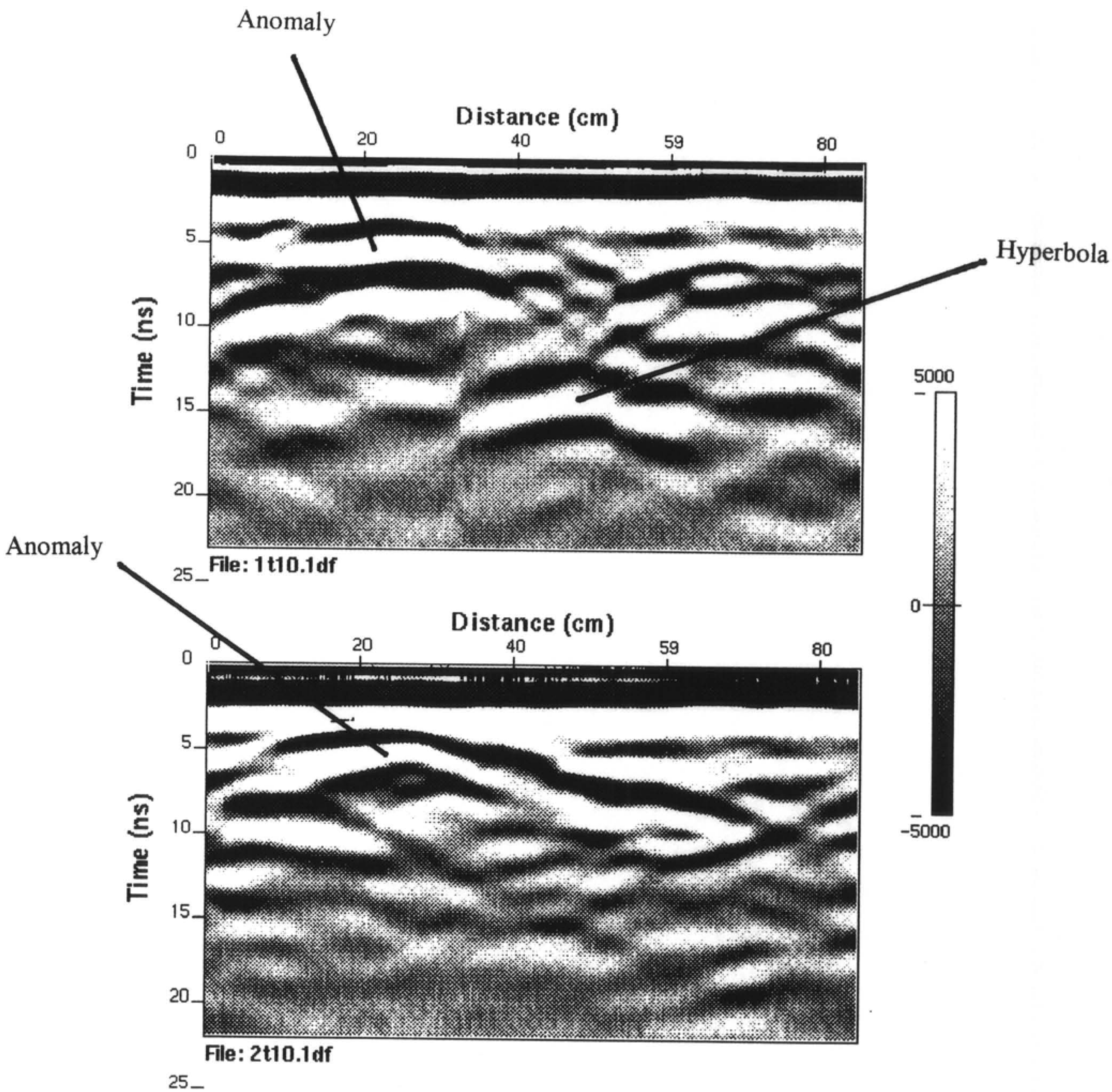

Figure 2. 2-D profile, line 10; co-pole antenna perpendicular to traverse direction and co-pole parallel to traverse direction

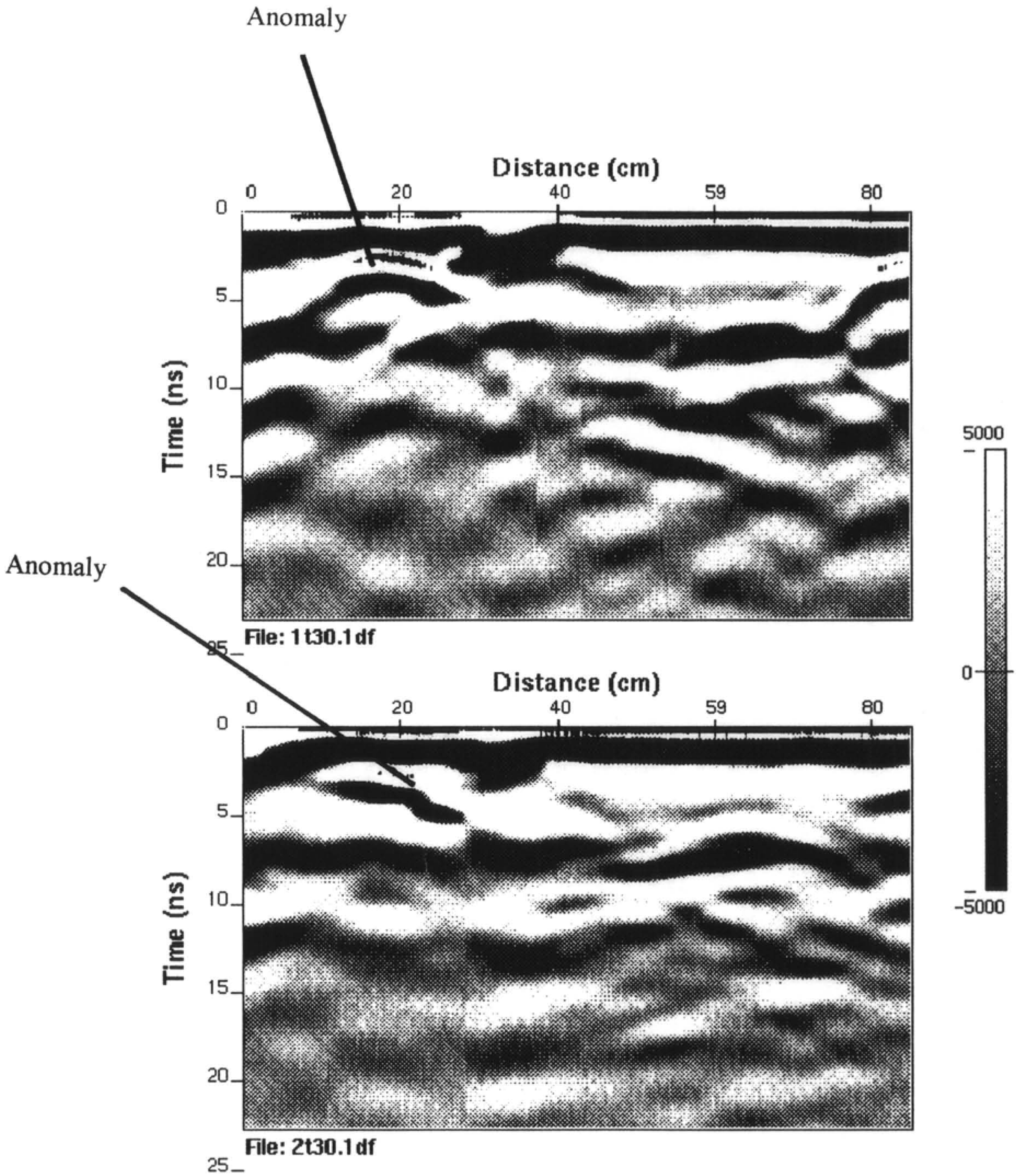

Figure 3. 2-D profile, line 30; co-pole antenna perpendicular to traverse direction and co-pole parallel to traverse direction

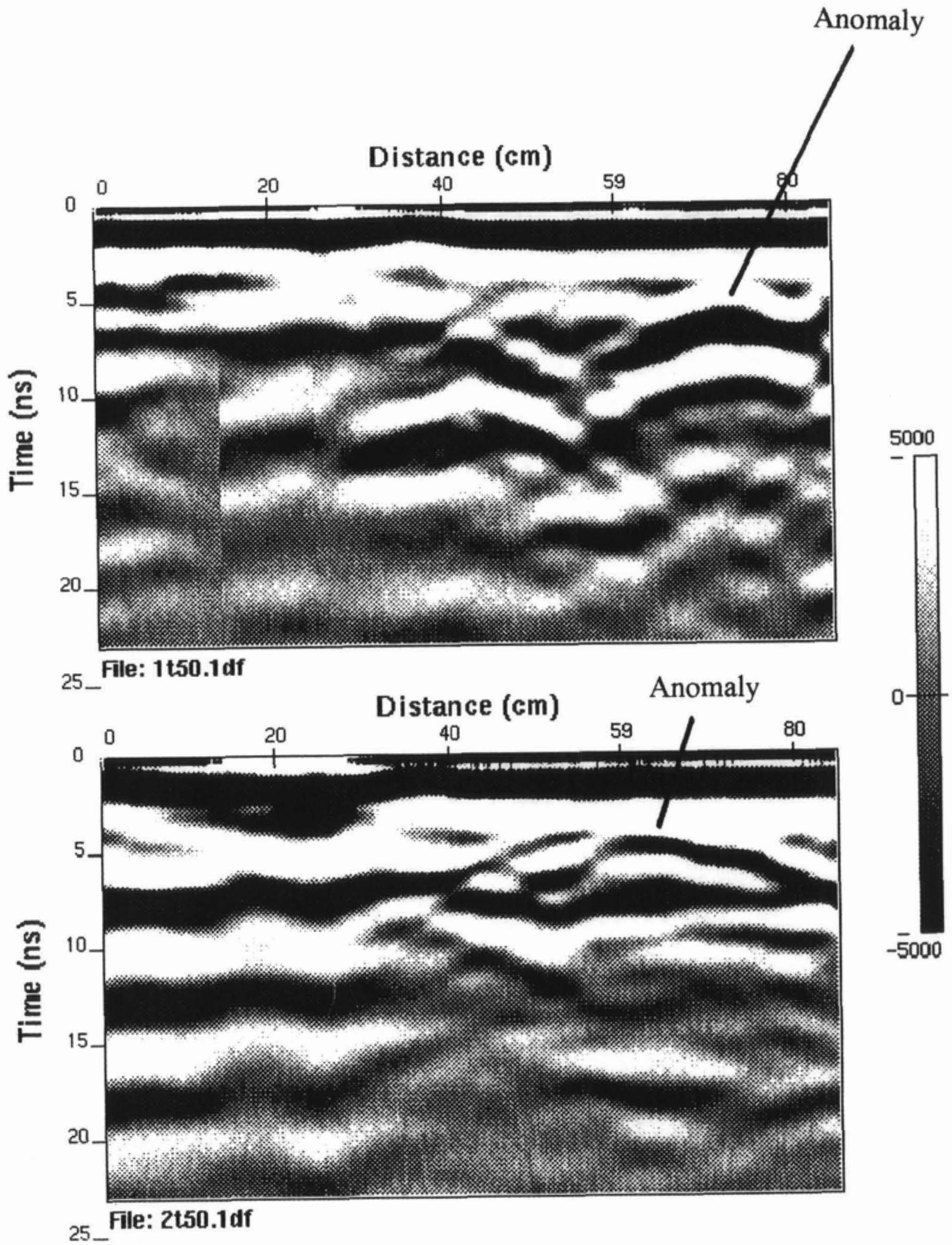

Figure 4. 2-D profile, line 50; co-pole antenna perpendicular to traverse direction and co-pole parallel to traverse direction

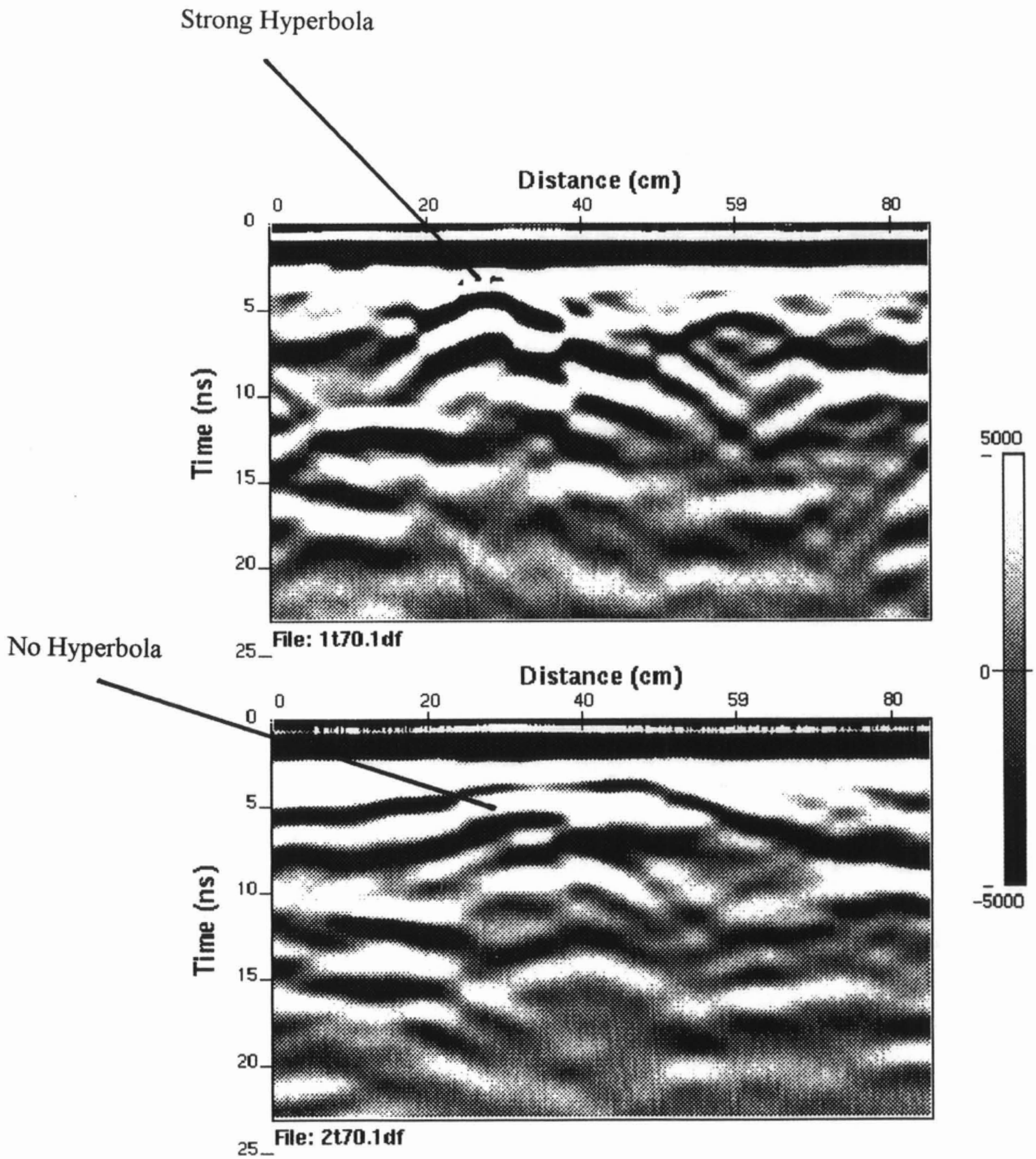

Figure 5. 2-D profile, line 70; co-pole antenna perpendicular to traverse direction and co-pole parallel to traverse direction

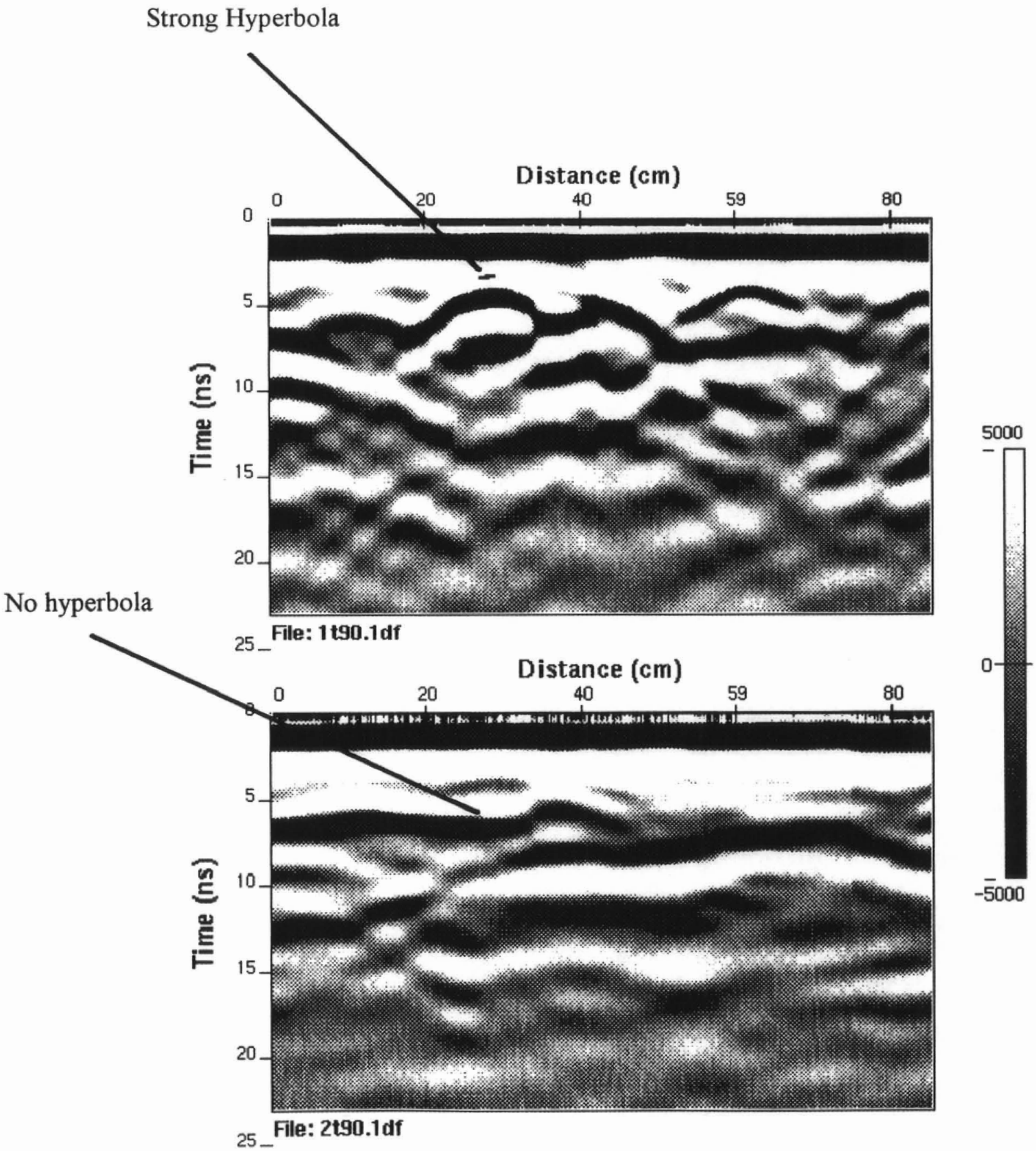

Figure 6. 2-D profile, line 90; co-pole antenna perpendicular to traverse direction and co-pole parallel to traverse direction

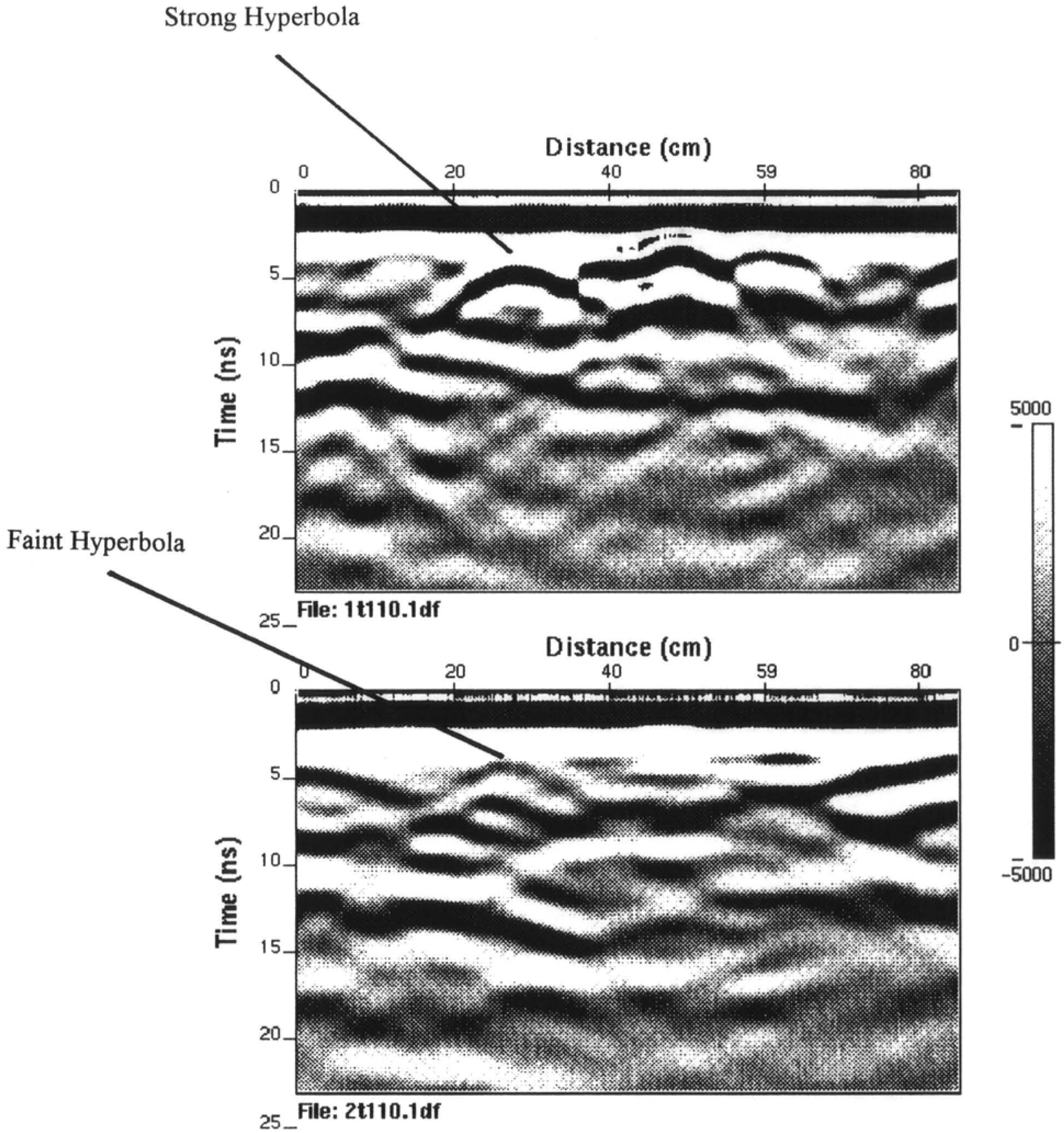

Figure 7. 2-D profile, line 110; co-pole antenna perpendicular to traverse direction and co-pole parallel to traverse direction

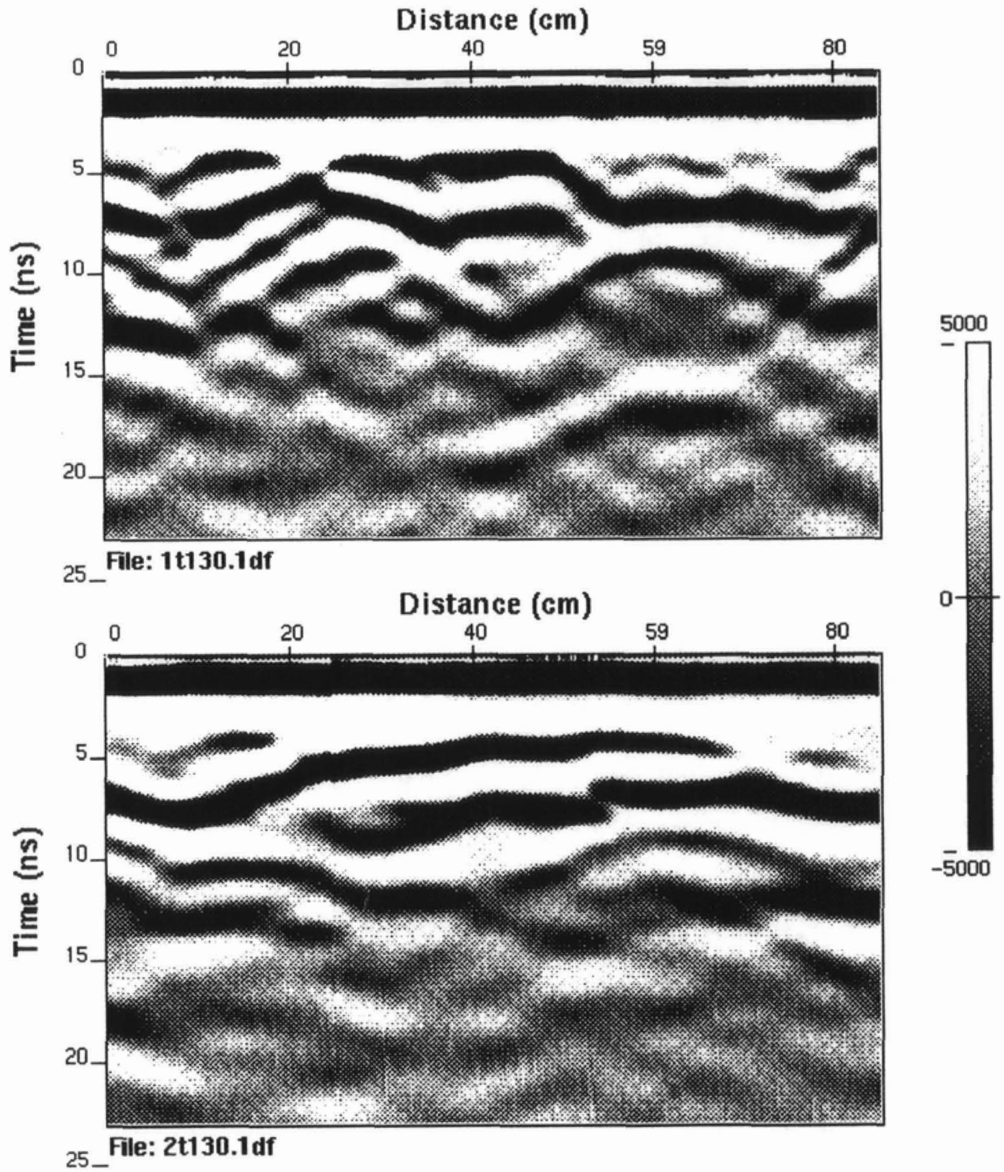

Figure 8. 2-D profile, line 130; co-pole antenna perpendicular to traverse direction and co-pole parallel to traverse direction

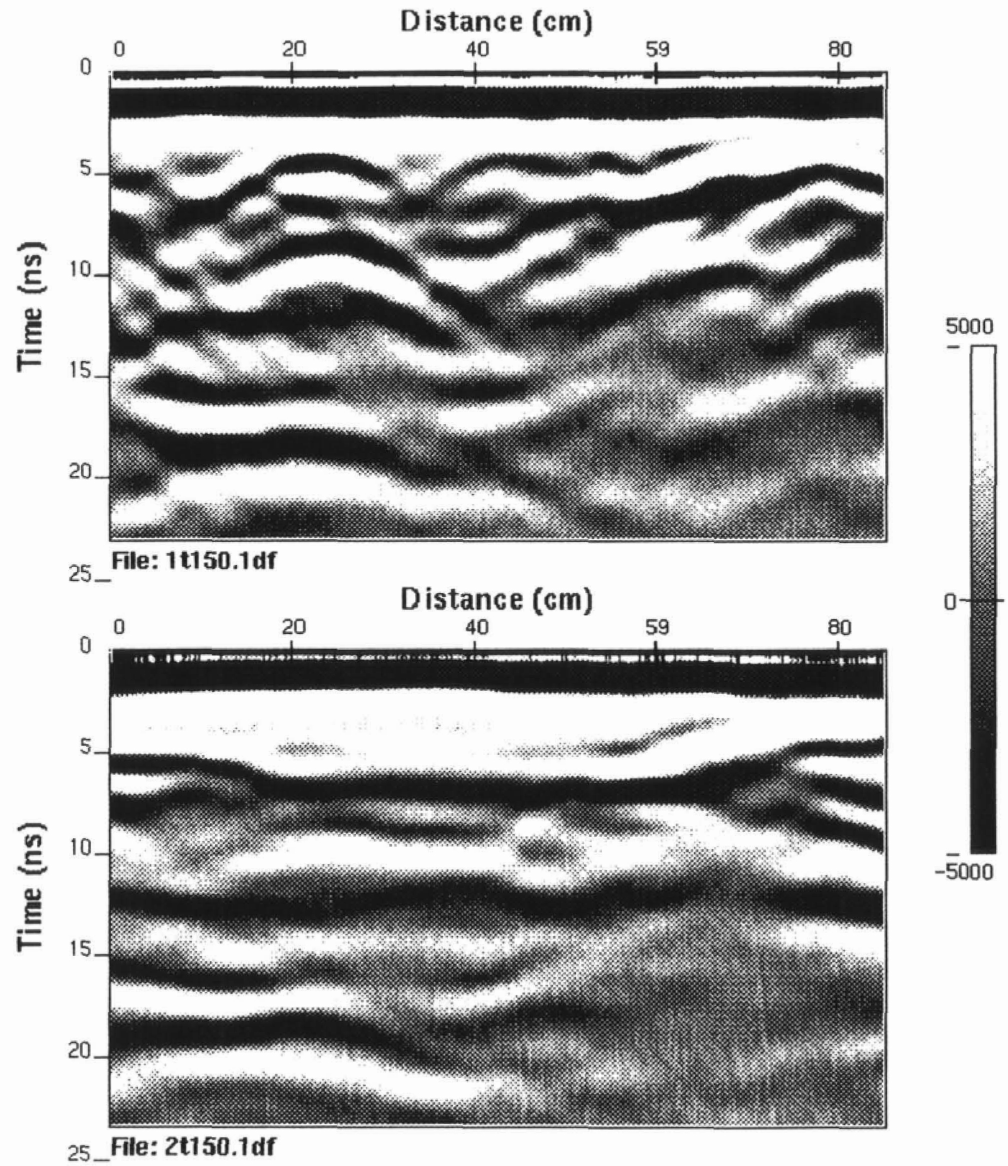

Figure 9. 2-D profile, line 150; co-pole antenna perpendicular to traverse direction and co-pole parallel to traverse direction

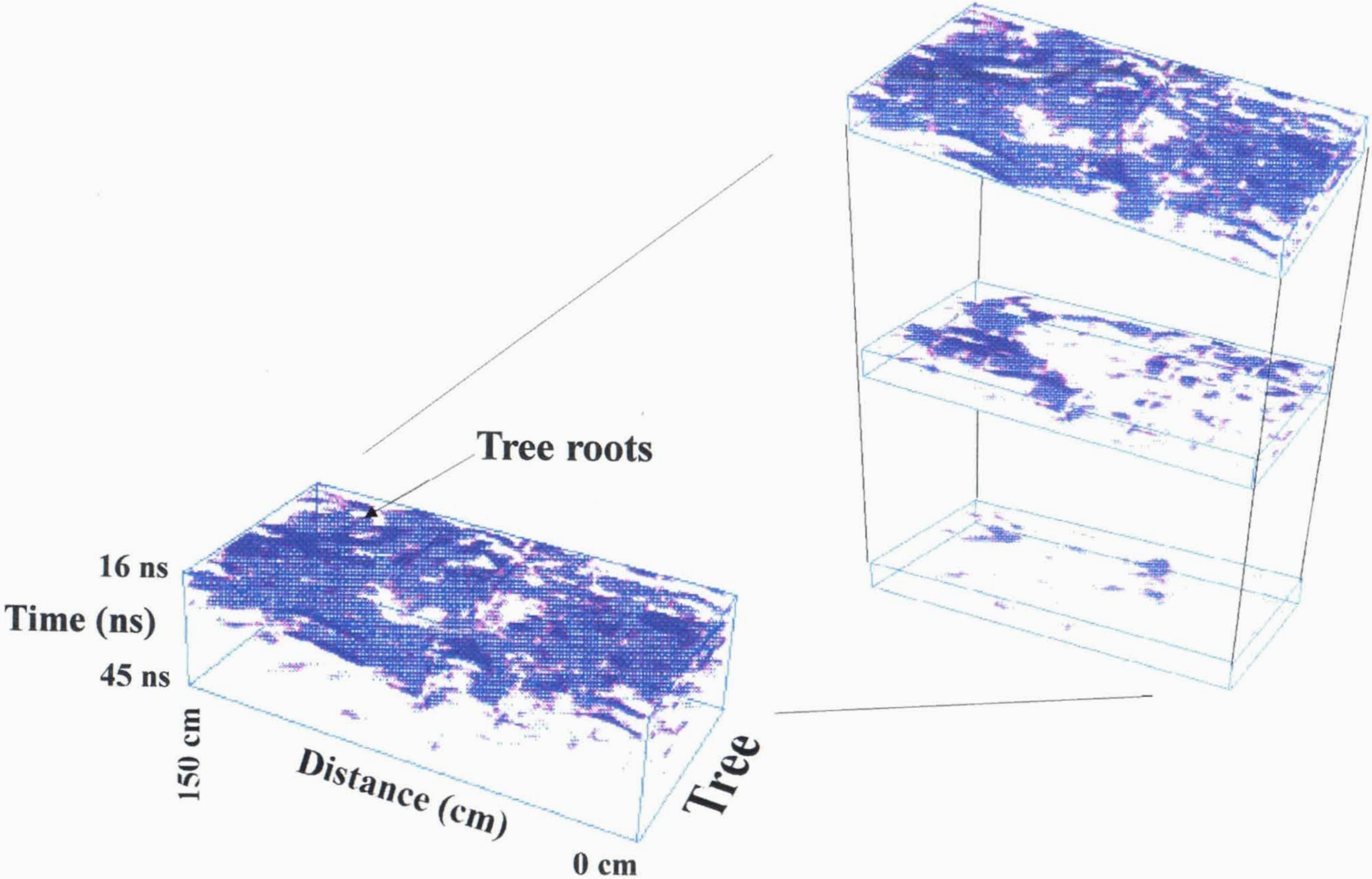

Figure 10. Co-pole perpendicular 3-D voxel based display

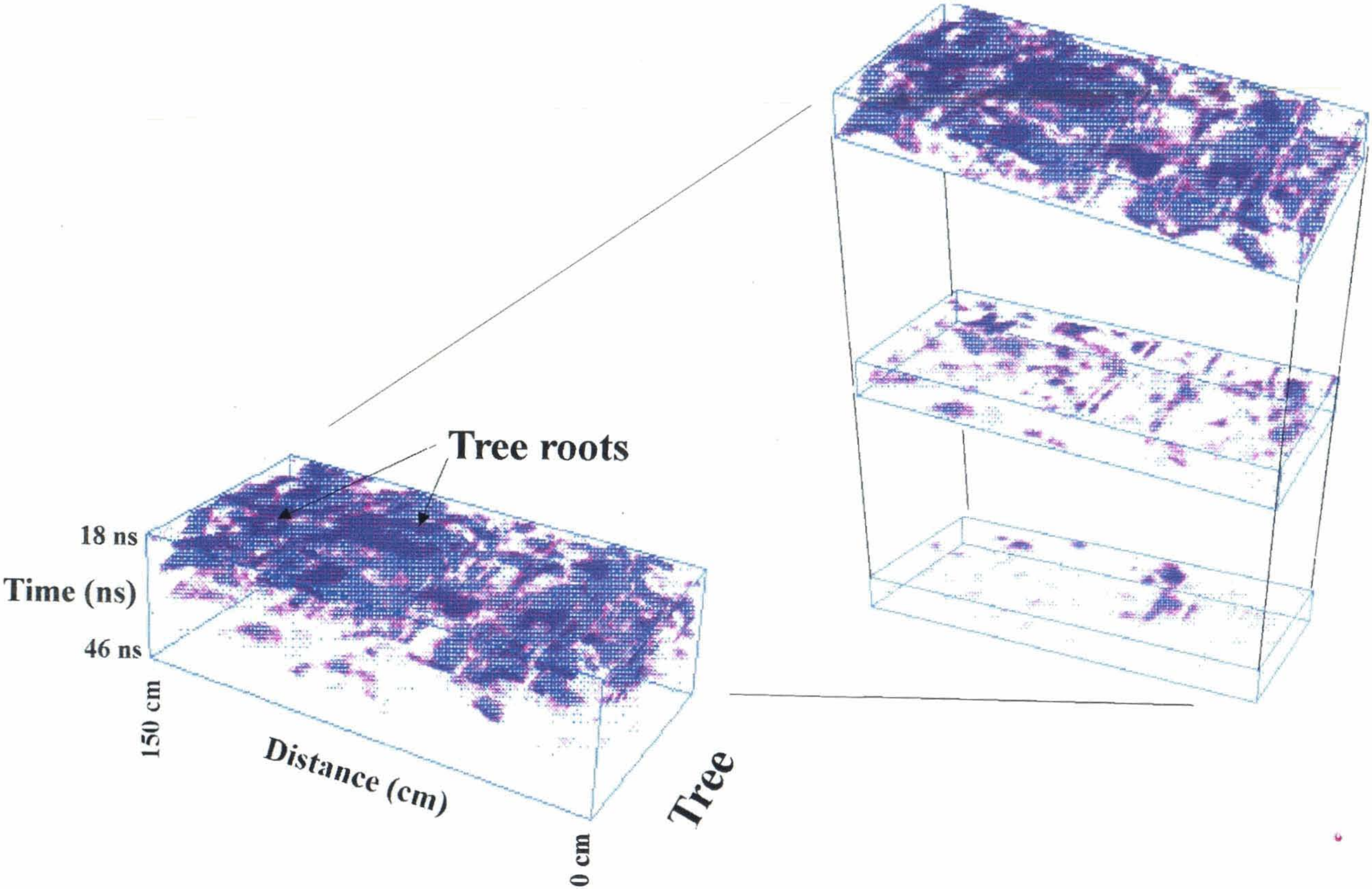

Figure 11. Co-pole parallel 3-D voxel based display.

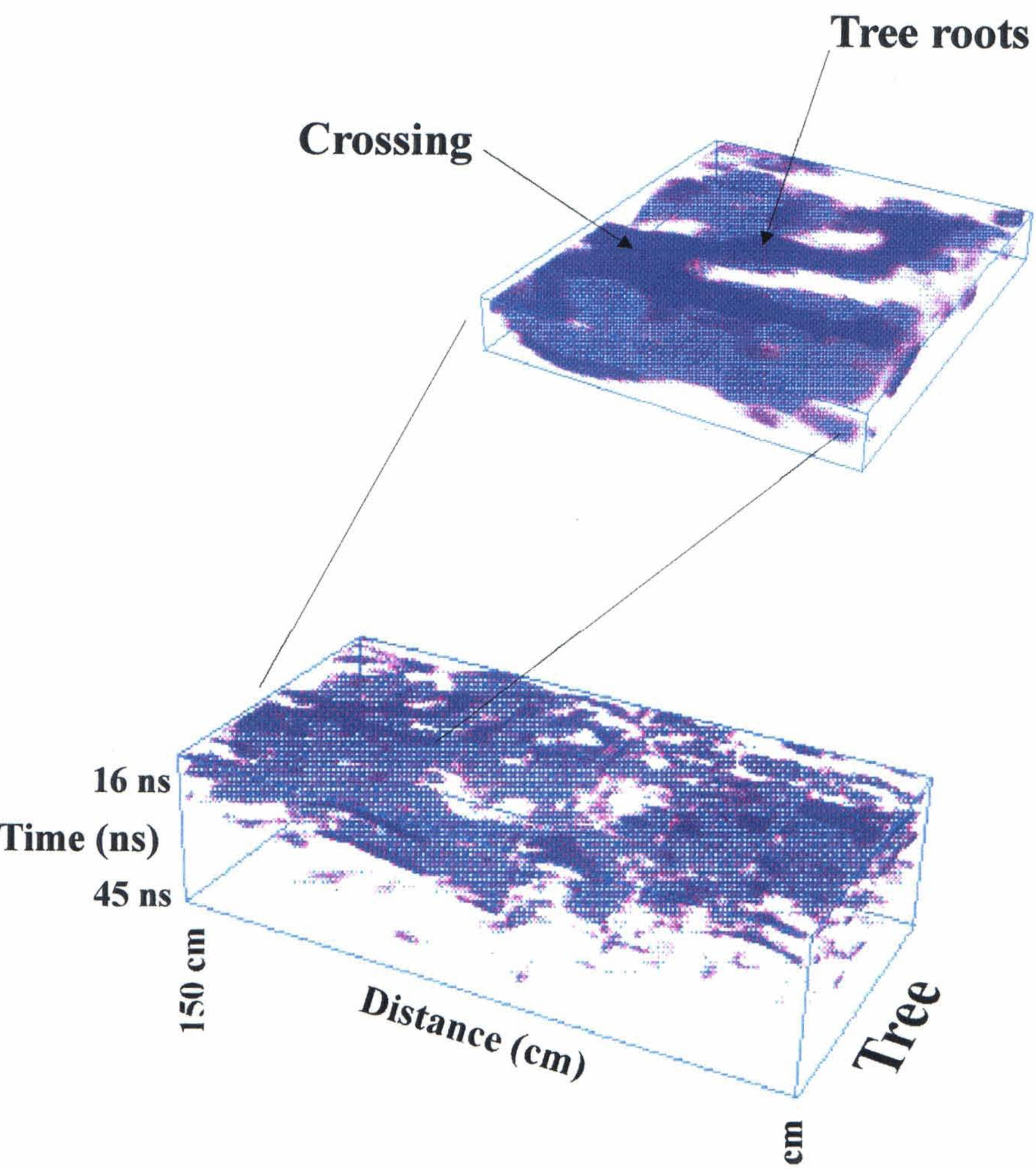

Figure 12. Co-pole perpendicular

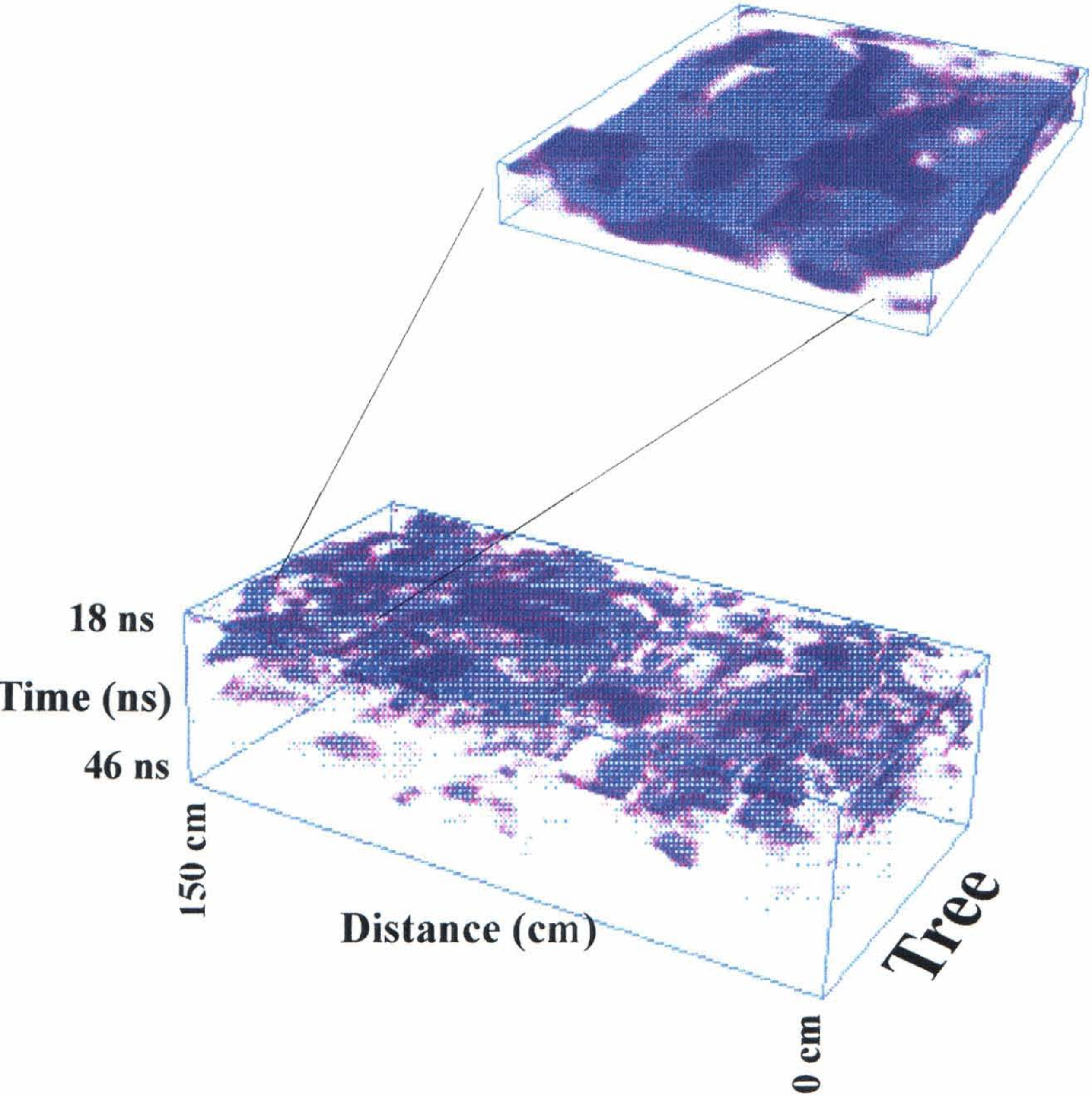

Figure 13. Co-pole parallel

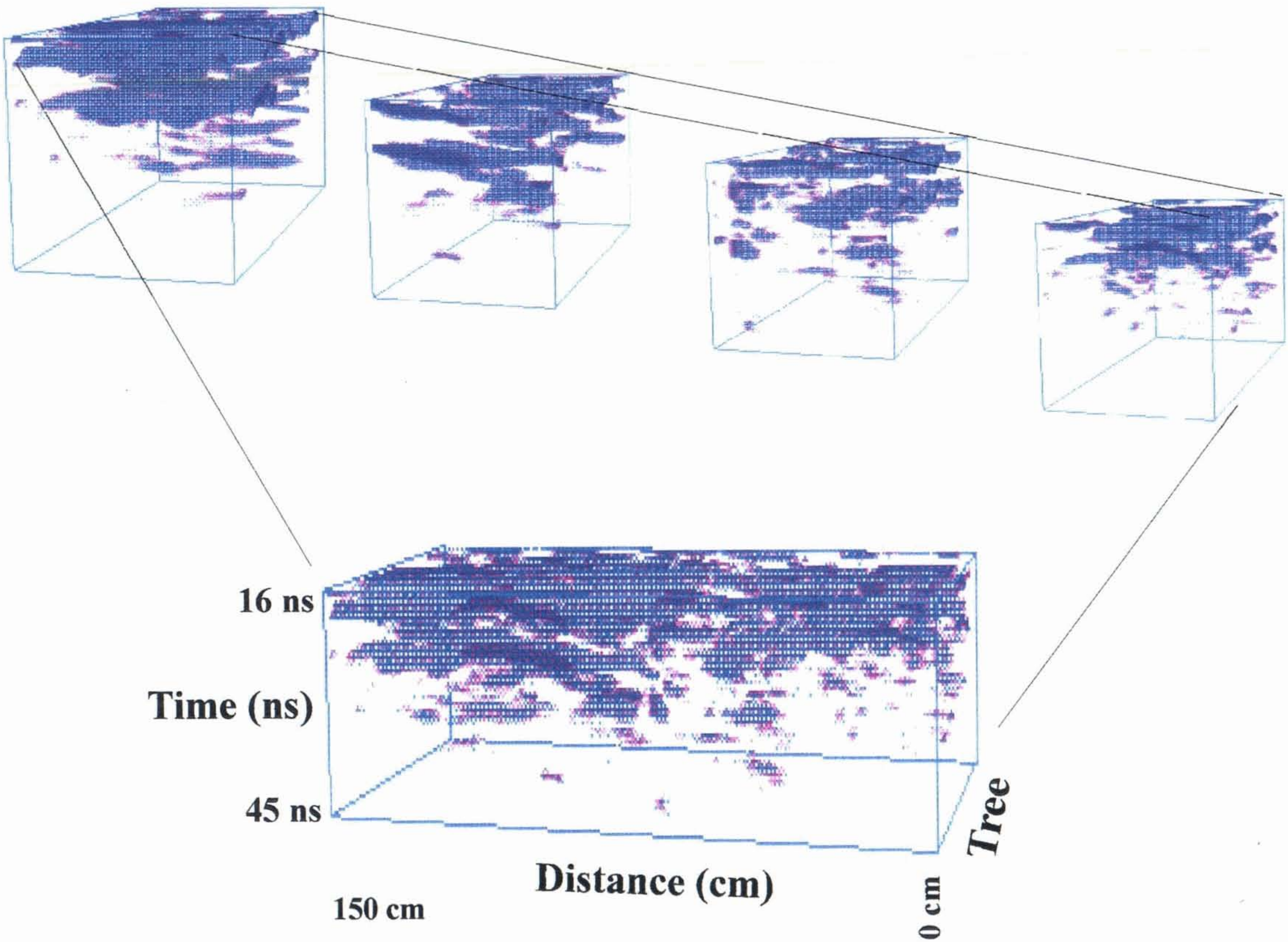

Figure 14. Co-pole perpendicular. Root depth increases away from tree